

## OCEAN SURFACE TOPOGRAPHY

Lee-Lueng Fu  
 Jet Propulsion Laboratory, California Institute of  
 Technology, Pasadena, CA, USA

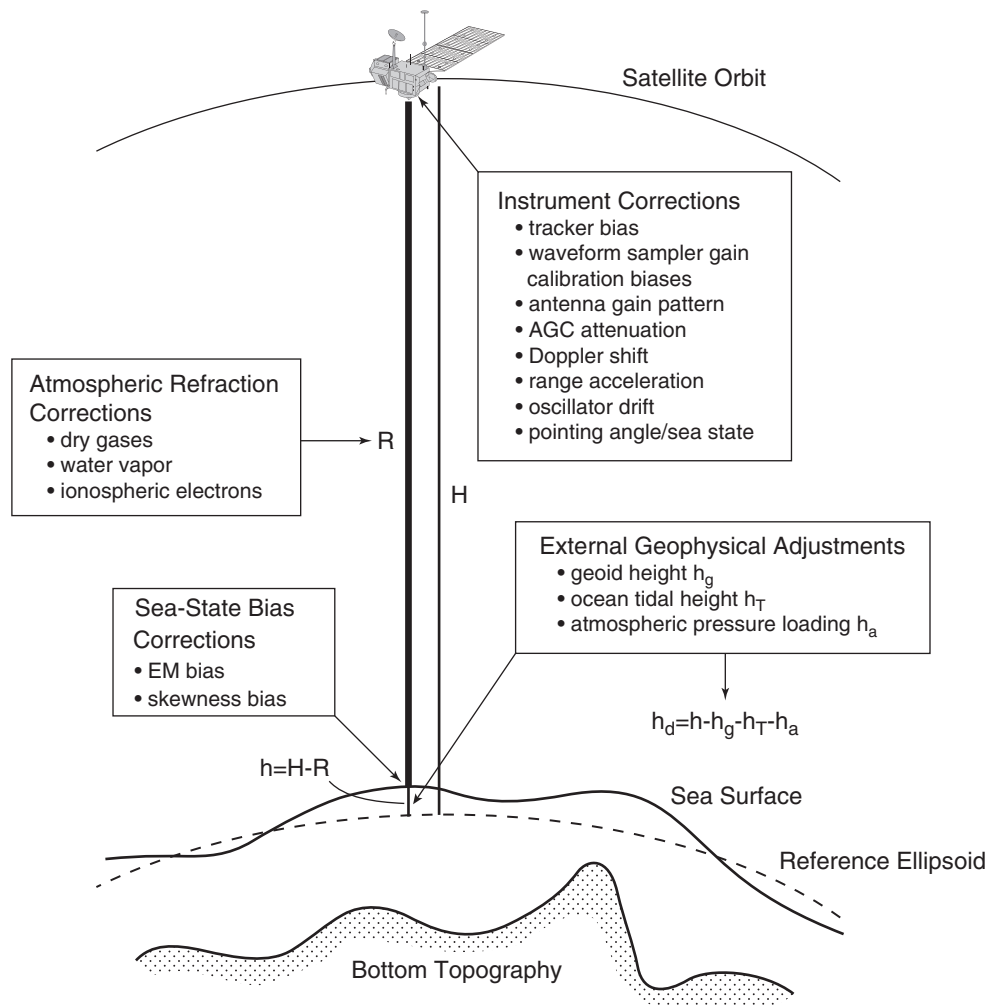
### Definition

The deviation of the height of the ocean surface from the geoid is known as the ocean surface topography. The geoid is a surface on which the Earth's gravity field is uniform. The ocean surface topography is caused by ocean waves, tides, currents, and the loading of atmospheric pressure. The main application of ocean surface topography is for the determination of large-scale ocean circulation.

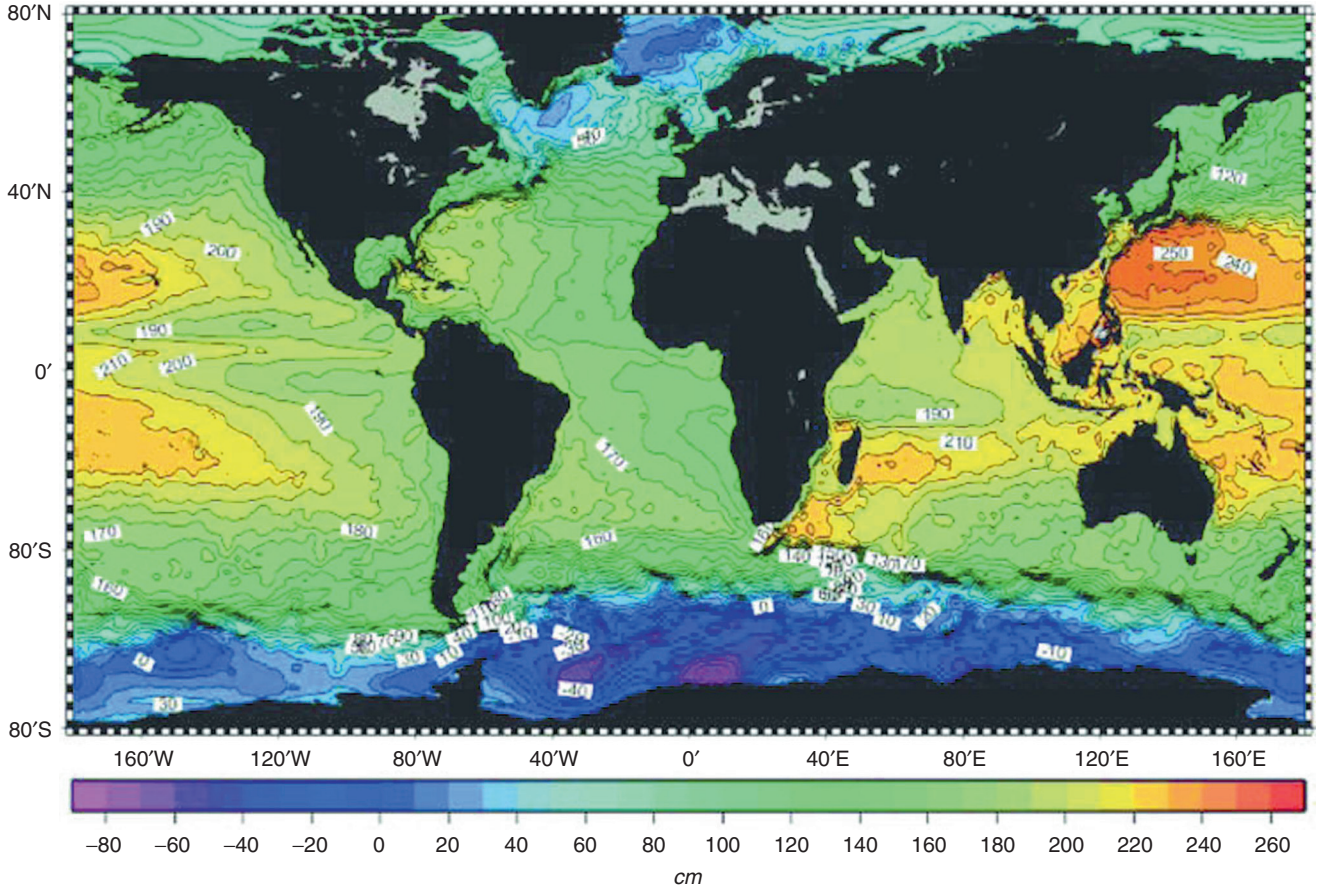
### Introduction

The determination of global ocean circulation has been a challenging goal of physical oceanographers. The fluid

motion of the ocean has a wide range of spatial and temporal scales. We all have the experience of watching ocean surface and being awed by the ever-changing waves and their breaking into turbulence and white caps. In order to measure the velocity of an ocean current, we must average out these wave effects. At longer periods, there are ocean tides. If the timescales of our interests are longer than tides, we must also average out the effects of tides. Fortunately, there is a dynamic property of large-scale ocean currents called the geostrophic balance. This balance occurs when the Rossby number, defined as  $U/fL$ , is much smaller than unity. In the notation,  $U$  is the speed of the current,  $L$  is the spatial scale, and  $f$  is the Coriolis parameter defined as  $f = 2\Omega \sin\phi$ , where  $\Omega$  is the Earth's rotation rate ( $7.292 \times 10^{-5}$  rad/s) and  $\phi$  is the latitude. For example, if  $U = 50$  cm/s at  $45^\circ$  latitude, geostrophic balance occurs when  $L \gg 5$  km. Then the geostrophic velocity of the current at ocean surface can be computed from the pressure at ocean surface as follows:



Ocean Surface Topography, Figure 1 Schematic illustration of the measurement system of satellite altimetry (From Chelton et al., 2001).



**Ocean Surface Topography, Figure 2** OST derived from a combined analysis of satellite altimeter data, surface drifter data, and a geoid model (From Rio and Hernandez, 2004).

$$fv = \frac{1}{\rho} \frac{\partial p}{\partial x} \quad (1)$$

$$fu = -\frac{1}{\rho} \frac{\partial p}{\partial y} \quad (2)$$

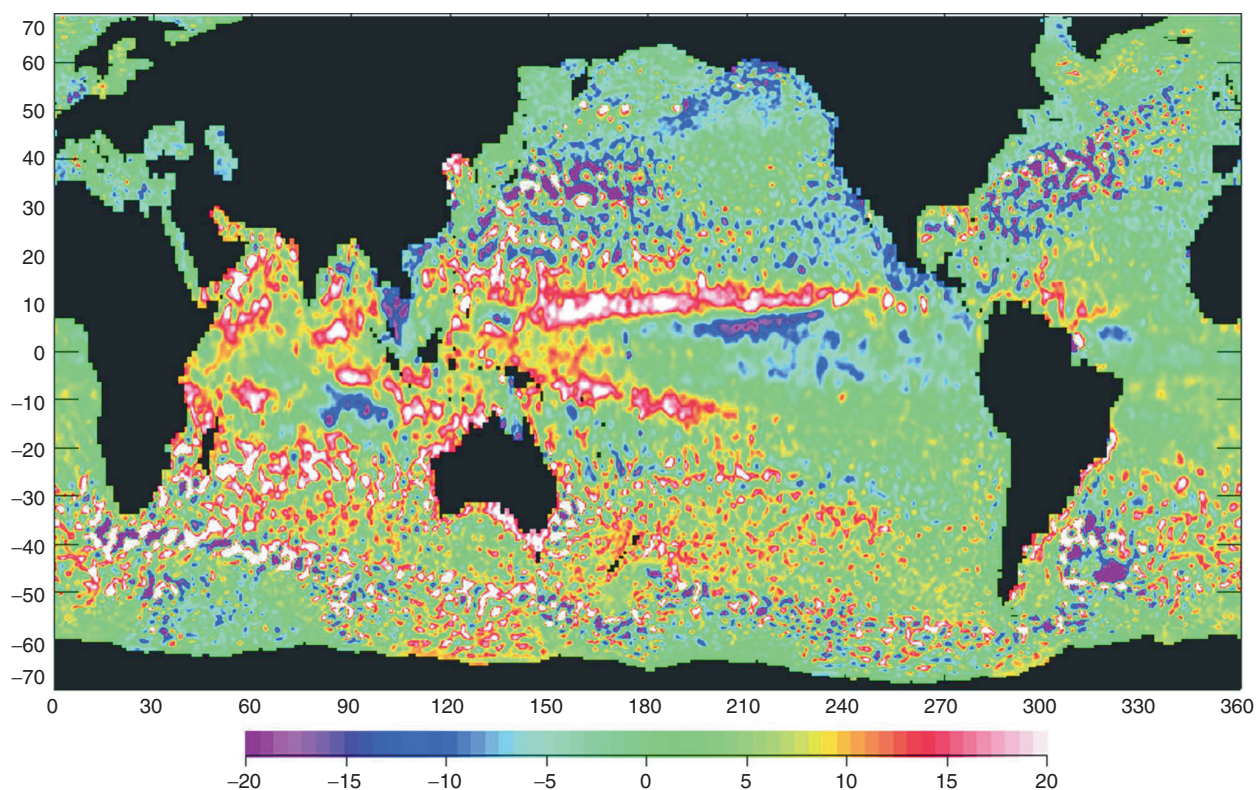
where  $p$  is the pressure,  $\rho$  is the density of sea water, and  $u$  and  $v$  are the zonal and meridional velocity components, respectively. The large-scale ocean currents are also in hydrostatic balance, namely,  $p = g \eta$ , where  $\eta$  is the elevation of the ocean surface topography (denoted by OST hereafter), defined as the deviation of the ocean surface from the geoid, and  $g$  is the Earth's gravity acceleration. The geoid is defined as the ocean surface on which the Earth's gravity field is uniform. In the absence of any motions, the ocean surface would be conformed to the geoid.

The role of OST for ocean currents is thus equivalent to the role of atmospheric surface pressure for winds. The speed and direction of large-scale wind blowing at

the Earth's surface can be computed from the gradient of the atmospheric surface pressure; similarly, the speed and direction of large-scale ocean surface currents can be computed from the gradient of OST as shown by Equations 1 and 2. OST has been traditionally estimated from the density field of the ocean as follows:

$$\eta_s = -\frac{1}{\rho_0} \left( \int_{-h}^0 \frac{\partial \rho}{\partial T} T' dz + \int_{-h}^0 \frac{\partial \rho}{\partial S} S' dz \right) \quad (3)$$

where  $T'$  and  $S'$  are the temperature and salinity deviations from their mean values, and  $\rho$  and  $\rho_0$  are the density and its depth average, respectively, and  $h$  is the depth of the ocean. This quantity,  $\eta_s$ , has been traditionally referred to as the steric sea level, which is an approximation of OST. In most places, the steric sea level is predominantly determined by temperature, and therefore is a good indicator of the heat content of the water column of the ocean. OST is also influenced by other factors such as



**Ocean Surface Topography, Figure 3** A snapshot (May 30, 2007) of the temporal change of OST from its time-mean value. The unit is cm.

wind, atmospheric pressure, and tides. However, our knowledge of OST has primarily been obtained through shipboard measurement of ocean temperature and salinity using Equation 3 until the recent development of satellite altimetry (Fu and Cazenave, 2001).

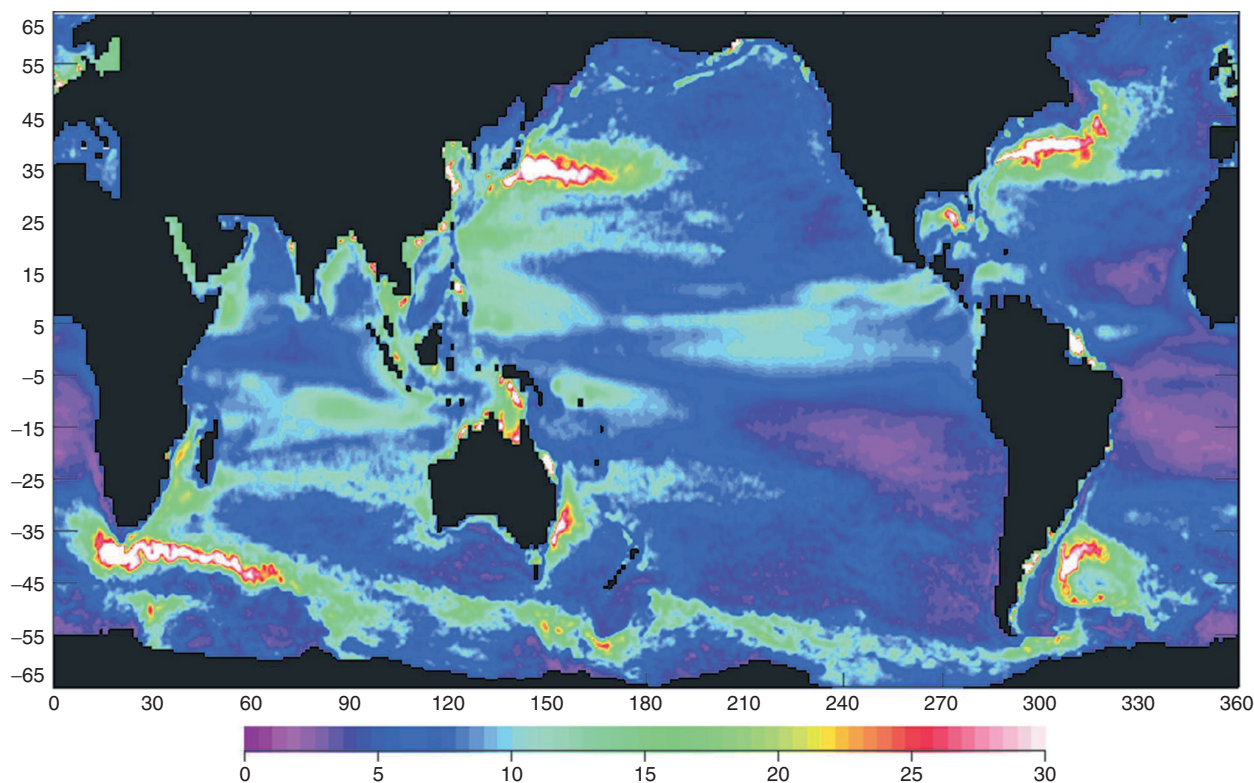
### Satellite altimetry

The concept of using a radar altimeter for measuring the height of sea surface was developed in the 1960s. The measurement of the round-trip travel time of a radar pulse from a satellite to the surface of the ocean allows the determination of the distance between the satellite and the ocean surface. If the location of the satellite in orbit is also known in an Earth-fixed coordinate, then the height of the sea surface is determined in this coordinate and so is the OST if the knowledge of the geoid is available as well. The first satellite altimeter was carried by Skylab launched in the early 1970s. The first satellite altimeter with sufficient precision for detecting OST was onboard Seasat, which was launched in 1978 returning only about 100 days of data. However, the first image of the ocean reflecting the variability of OST caused by ocean currents provided a revolutionary impact on the

oceanography community. Oceanographers began to realize the potential of observing the global ocean circulation from OST determined from space.

The challenges of determining OST from satellite altimetry were the measurement accuracies. For example, an error of 1 cm in OST is capable of producing an error in the mass transport by ocean current of the magnitude of several million tons per second, which is a significant fraction of the transport of major ocean currents. The technique of satellite altimetry is conceptually straightforward, but there are numerous sources for measurement errors as illustrated in Figure 1. Corrections for these errors constitute the enterprise of precision altimetry beginning with the TOPEX/Poseidon Mission. The reader is referred to Chelton et al. (2001) for a treatise of the details. Only the major components of the measurement system are briefly described in this entry.

First, the free electrons in the Earth's ionosphere slow down the radar signals and have a net effect of more than 20 cm in error if not corrected. To correct for this error, radar altimeter must transmit in two channels, for example, the Ku band (13.6 GHz) and the C band (5.3 GHz) as the TOPEX/Poseidon altimeter. The signal delays are different for the measurements made at the two channels, which are used



**Ocean Surface Topography, Figure 4** The standard deviation of the temporal change of OST in unit of centimeters.

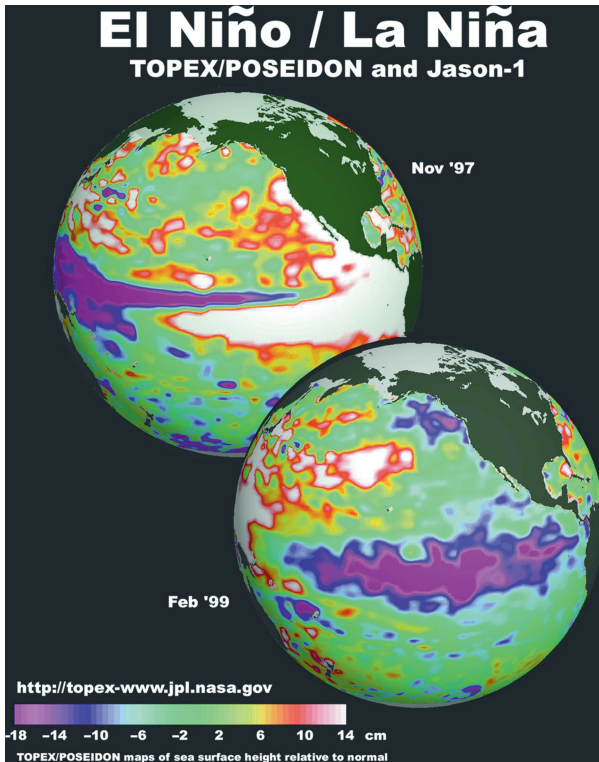
to determine the total electron content and the signal delay. Second, the water vapor in the Earth's troposphere also has the effect of delaying radar signals by more than 40 cm in the tropics. The approach of the TOPEX/Poseidon Mission was to carry a three-frequency microwave radiometer for making measurement of the water vapor content and the corresponding signal delay of the altimeter. Third, the precise location of the satellite in orbit must be determined. This requires onboard precision tracking systems and well-maintained geodetic ground systems. For example, the TOPEX/Poseidon Mission carries three independent orbit tracking systems: laser retroreflectors, GPS receivers, and a Doppler system called DORIS.

After Seasat, there were two satellite altimeters flown without the full suite of capabilities of error corrections: the US Geosat and the European Remote-Sensing Satellite (ERS). The first satellite altimeter mission that was dedicated to optimal measurement of OST was the joint American/French TOPEX/Poseidon Mission, launched in 1992. Aside from the complete measurement system, the  $66^\circ$  orbit inclination was chosen for the determination of ocean tides, and the 1336 km orbit altitude was chosen for precision orbit determination. The results from the mission have revolutionized the study of global ocean circulation from the OST determined from the mission and its follow-on, the Jason Mission, which was launched in 2001. Jason-2 was launched in 2008 to succeed Jason-1

to continue the precision altimetry data record. In the mean time, the other satellite altimeters from the ERS, ENVISAT, and Geosat Follow-On (GFO) missions have contributed to the measurement of sea surface height and OST by providing enhanced spatial and temporal resolutions. These missions have, however, benefited from the cross-calibration with the precision missions for correcting for large-scale errors such as orbit errors and tidal effects. It has been recognized by the altimetry community that the continuation of precision missions (e.g., Jason) in combination with other missions (e.g., ENVISAT) is essential for the measurement of OST for a variety of applications.

### Ocean general circulation

The measurement of sea surface height from satellite altimetry is not sufficient for the determination of OST. The missing link is the geoid. Direct measurement of the Earth's gravity field for geoid determination is limited to a resolution of 300 km at present (Jayne, 2000). The OST derived from subtracting the geoid from the altimetry sea surface height data is thus lacking accurate information at smaller scales. In order to obtain OST with sufficient resolution to reveal the detailed features of the ocean general circulation such as the Gulf Stream and other ocean current systems, we have to supplement the satellite-derived result



**Ocean Surface Topography, Figure 5** Maps of the temporal change of the OST of the Pacific ocean during the 1997 El Niño (*upper globe*) and the 1999 La Niña (*lower globe*).

with information derived from in situ measurements of ocean current velocity and density field. Displayed in Figure 2 is a map of time-averaged global OST estimated from combined data from satellite and in situ measurements (Rio and Hernandez, 2004). The spatial gradient of OST reveals the patterns of the ocean general circulation. The concentration of OST contours in major ocean current systems is clearly shown: the Gulf Stream in the western North Atlantic, the Kuroshio (or the Japan Current) in the western North Pacific, and the Antarctic Circumpolar Current around Antarctica. The data used for constructing the map were collected during the period 1993–1999, which is relatively short for representing the time-averaged ocean general circulation. Many of the details of OST and its gradient cannot be determined to be permanent features or manifestations of unaveraged temporal variability of ocean currents. Nevertheless, Figure 2 represents an estimate of the steady state of OST based on a state-of-the-art set of modern observations.

### Mesoscale variability

Displayed in Figure 3 is an instantaneous map showing the temporal change of the OST from its time-averaged value shown in Figure 2. The map is constructed from a merged product from the altimeter data of the TOPEX/Poseidon and the ERS satellites

(Ducet et al., 2000). It is apparent that the spatial scales of the temporal variability in the tropics are much larger than those at the mid- and high latitudes, where the variability is dominated by the mesoscales with wavelengths shorter than 500 km. This mesoscale variability is the ocean's analog of the storms in the atmosphere. These mesoscale eddies are primarily created by the instability of ocean currents. They have maximum strength near the major current systems of the ocean, as illustrated by Figure 4 which is a map of the standard deviation of the OST calculated from the same merged data. The standard deviation of OST is a measure of the intensity of the ocean eddy field, which contains 90 % of the kinetic energy of ocean circulation and plays a significant role in transporting heat, salt, dissolved gases (e.g., CO<sub>2</sub>), and nutrients around the global oceans.

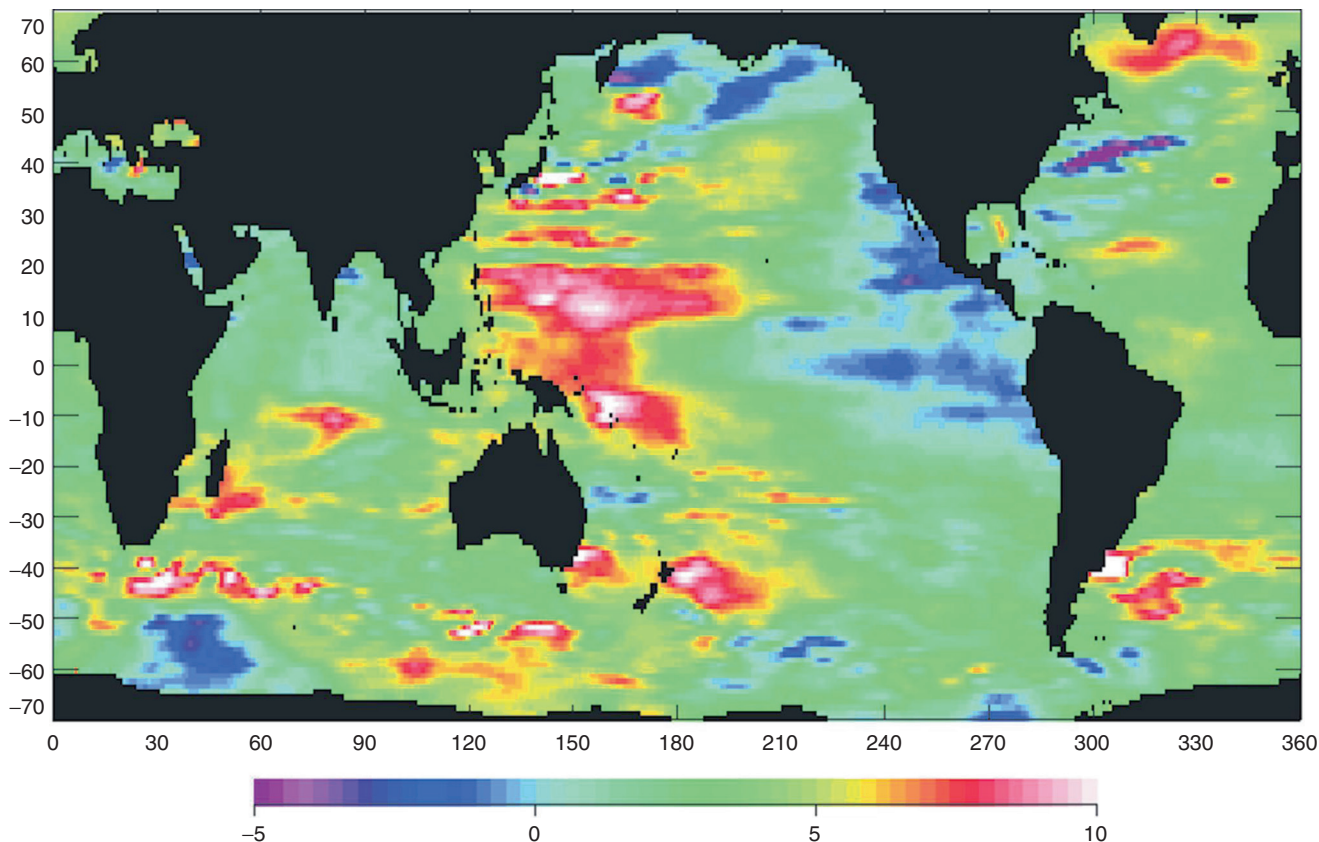
### Basin-scale variability

The strongest variability at the scales of the ocean basins takes place in the tropics, as illustrated by the features in the Pacific Ocean and the Indian Ocean in Figure 3. In the Pacific Ocean, the tropical region is characterized by a seesaw pattern of exchange of heat between the western and eastern parts of the ocean resulting from an ocean–atmosphere coupled climatic system. When the heat content is anomalously high in the eastern and central tropical Pacific with OST higher than normal by up to 30 cm, the condition is called El Niño; when the heat content is anomalously low there with low OST, the condition is called La Niña (see Figure 5). The tropical Pacific is in these alternating states every 2–7 years with worldwide impact on weather and climate.

The basin-scale variability at mid- and high latitudes is quite different from that in the tropics. At high frequencies (with periods less than a season), such variability has a magnitude of generally less than 10 cm caused by the fluctuations of the volume of water mass in the entire water column driven by wind and atmospheric pressure at timescales of days to weeks. At low frequencies (with periods of a season and longer), the variability is associated with the seasonal, interannual, and decadal variability of the ocean. The forcing is a combination of thermal, hydrological, and wind origin. Displayed in Figure 6 is the geographic pattern of the linear trend of the temporal change in OST estimated from satellite altimetry data collected in the period from 1993 to 2008. The timescales of the variability are on the order of a decade, reflecting the climatic change of the ocean circulation and the global sea level. Note that the sea level in most regions of the global ocean is rising, causing a global mean sea level rise at a rate of 3.3 mm/year. Part of the rise is caused by the warming of the ocean that expands the volume of sea water, and the other part is caused by the melting of ice on land that adds water to the global oceans.

### Practical applications

The information obtainable from OST on the circulation and the heat content of the ocean finds many practical



**Ocean Surface Topography, Figure 6** The linear trend of temporal change of OST from 1993 to 2008. The unit is mm/year.

applications. For example, the fluctuations of ocean current velocity in the Gulf of Mexico have important effects on the safety and operational cost of the offshore oil drilling industry in the region. The data product of OST and current velocity has been made available to the offshore operators, resulting in cost savings of up to a half million US dollars in a single operation involving towing oil rigs along optimal routes. The upper ocean heat storage estimated from OST has proven useful for the prediction of the strength of hurricanes. This is because a hurricane draws its energy for growth from the heat stored below the sea surface. While the information of sea surface temperature reflects the heat only in a thin layer of the ocean surface, the heat stored below the ocean surface estimated from OST contains the fuel for hurricane to grow. Other applications include El Niño and La Niña predictions, fisheries management, marine mammal research, ship routing, and monitoring global sea level rise.

### Outlook

We have come a long way since the first global OST observed from Seasat. The observations from all the satellite altimeters have since revolutionized the fields of

oceanography and geodesy, as well as created many practical applications. However, there is a significant limitation in the conventional radar altimetry. The size of the pulse-limited radar footprint underlying the conventional radar altimetry increases from 2 to 10 km with the height of ocean waves. Even with thousands of pulses averaged over a second, the measurement noise over the large footprint has limited the spatial resolution of altimeter observation to wavelengths longer than 100 km. A major fraction of the ocean's kinetic energy is contained at wavelengths shorter than 100 km. Furthermore, the dissipation of ocean energy and the associated stirring and mixing of ocean properties like temperature and carbon dioxide content are controlled by physical processes at these short wavelengths. Many of the ocean processes in the coastal zones like the upwelling of nutrients, currents, fronts, and eddies that affect offshore operation, navigation, and waste disposal also have small scales that cannot be resolved by the conventional altimeter measurements.

A new technology of radar interferometry coupled with synthetic-aperture technique offers the opportunity of making high-resolution wide-swath measurement of OST (Fu and Rodriguez, 2004). This approach has been demonstrated by the Shuttle Radar Topography Mission

for mapping the land topography (Farr et al., 2007). By operating at a frequency above 30 GHz and a look angle of 4°, the concept of a wide-swath altimeter mission based on SAR interferometry has been proposed for mapping OST as well as the elevation of the water levels of rivers and lakes. A satellite mission with this capability will make breakthroughs in both ocean dynamics and land hydrology, which hold the key to understanding the evolving climate change as well as to monitoring and mitigating its consequences. Such a satellite mission called Surface Water and Ocean Topography (SWOT) has recently been established by a joint effort of the USA and France with contributions from Canada. SWOT is currently planned for launch in 2020.

### Acknowledgment

This research was carried out at the Jet Propulsion Laboratory, California Institute of Technology, under a contract with the NASA.

### Bibliography

- Chelton, D. B., Ries, J., Haines, B., Fu, L.-L., and Callahan, P., 2001. Satellite altimetry. In Fu, L.-L., and Cazenave, A. (eds.), *Satellite Altimetry and Earth Sciences: A Handbook for Techniques and Applications*. San Diego: Academic, pp. 1–131. 423.
- Ducet, N., Le Traon, P. Y., and Reverdin, G., 2000. Global high resolution mapping of ocean circulation from the combination of TOPEX/POSEIDON and ERS-1/2. *Journal of Geophysical Research (Oceans)*, **105**(C8), 19477–19498.
- Farr, T. G., Rosen, P. A., Caro, E., Crippen, R., Duren, R., Hensley, S., Kobrick, M., Paller, M., Rodriguez, E., Roth, L., Seal, D., Shaffer, S., Shimada, J., Umland, J., Werner, M., Oskin, M., Burbank, D., and Alsdorf, D., 2007. The shuttle radar topography mission. *Reviews of Geophysics*, **45**, RG2004, doi:10.1029/2005RG000183.
- Fu, L.-L., and Cazenave, A. (eds.), 2001. *Satellite Altimetry and Earth Sciences: A Handbook of Techniques and Applications*. San Diego: Academic, p. 463. 463.
- Fu, L.-L., and Rodriguez, R., 2004. High-resolution measurement of OST by radar interferometry for oceanographic and geophysical applications. In Sparks, R. S. J., and Hawkesworth, C. J. (eds.), *State of the Planet: Frontiers and Challenges*. Washington, DC: American Geophysical Union. AGU Geophysical Monograph 150, IUGG, Vol. 19, pp. 209–224.
- Jayne, S. R., 2006. Circulation of the north Atlantic ocean from altimetry and the gravity recovery and climate experiment geoid. *Journal of Geophysical Research*, **111**, C03005, doi:10.1029/2005JC003128, 2006.
- Rio, M.-H., and Hernandez, F., 2004. A mean dynamic topography computed over the world ocean from altimetry, in situ measurements, and a geoid model. *Journal of Geophysical Research*, **109**, C12032, doi:10.1029/2003JC002226.

### Cross-references

Climate Data Records  
 Geodesy  
 Ocean Modeling and Data Assimilation  
 Ocean, Measurements and Applications  
 Radar, Altimeters  
 Sea Level Rise

## OCEAN SURFACE VELOCITY

Bertrand Chapron<sup>1</sup>, Johnny Johannessen<sup>2</sup> and Fabrice Collard<sup>3</sup>

<sup>1</sup>Satellite Oceanography Laboratory, IFREMER, Plouzané, France

<sup>2</sup>Nansen Environmental and Remote Sensing Center, Bergen, Norway

<sup>3</sup>CLS, Division Radar, Plouzané, France

### Synonyms

Doppler; Surface velocity; Synthetic aperture radar

### Definition

*Doppler shift anomaly*. Residual signal Doppler frequency from geometrically predicted Doppler frequency

*Range Doppler velocity*. Velocity conversion from Doppler shift anomaly estimate

### Introduction

Regular repeat global measurements of absolute surface currents as well as ageostrophic processes including convergence and divergence along meandering fronts and eddies at scales smaller than 30 km are rare.

To derive global ocean surface current estimates from space, the basic tool is the radar altimeter. High-class altimeters (TOPEX, JASON, ERS, ENVISAT) are indeed measuring the oceanographic surface topography with good precision. Ocean surface current estimates are then retrieved assuming a linear balance between the gradient of the sea surface topography and surface geostrophic current. Satellite altimetry is a very mature satellite remote sensing technique with an extensive literature describing advances in knowledge and understanding of ocean circulation.

Satellite altimetry has in particular been suited to infer the statistical characterization of mesoscale variability. Thanks to its global, repeat, and long-term sampling, the estimation of sea surface height (SSH) wave number spectra has been a unique contribution of satellite altimetry to quantitative assessment of spectral slopes at scales ranging from about 50 to 100 km up to a spectral peak that generally emerges at twice the wavelength of the internal deformation radius (i.e., 300–400 km at mid-latitudes). Presently, assimilation of altimetry sea level anomaly (SLA) is routinely applied in several ocean modeling and forecasting systems. As such the availability and continuity of altimetric measurements are essential for operational oceanography. Yet, the finer-scale (less than 50 km) oceanic mesoscale and submesoscale energy is difficult to map with conventional radar altimeters because of the narrow illuminated swath, regardless of the orbital configuration.

Mesoscale and submesoscale processes are recognized for their importance and impact on biogeochemical processes and mixing, on air-sea interactions, and for the transfer of energy between scales. To adequately resolve



<http://www.springer.com/978-0-387-36698-2>

Encyclopedia of Remote Sensing

Njoku, E.G. (Ed.)

2014, XXV, 939 p. 370 illus., 223 illus. in color.,

Hardcover

ISBN: 978-0-387-36698-2